BIOCHEMISTRY
including biophysical chemistry & molecular biology

Article

pubs.acs.org/biochemistry

Effect of Basic Cell-Penetrating Peptides on the Structural, Thermodynamic, and Hydrodynamic Properties of a Novel Drug Delivery Vector, ELP[$V_5G_3A_2$-150]

Daniel F. Lyons,[†] Vu Le,[‡] Wolfgang H. Kramer,[§] Gene L. Bidwell, III,[∥] Edwin A. Lewis,[‡] Drazen Raucher,[†] and John J. Correia*[,†]

[†]Department of Biochemistry, University of Mississippi Medical Center, 2500 North State Street, Jackson, Mississippi 39216, United States

[‡]Department of Chemistry, Mississippi State University, Mississippi State, Mississippi 39762, United States

[§]Department of Chemistry and Biochemistry, Millsaps College, 1701 North State Street, Jackson, Mississippi 39210, United States

[∥]Department of Neurology, University of Mississippi Medical Center, 2500 North State Street, Jackson, Mississippi 39216, United States

Supporting Information

ABSTRACT: Elastin-like polypeptides (ELPs) are large, nonpolar polypeptides under investigation as components of a novel drug delivery system. ELPs are soluble at low temperatures, but they desolvate and aggregate above a transition temperature (T_T). This aggregation is being utilized for targeting systemically delivered ELP−drug conjugates to heated tumors. We previously examined the structural, thermodynamic, and hydrodynamic properties of ELP[$V_5G_3A_2$-150] to understand its behavior as a therapeutic agent. In this study, we investigate the effect that adding basic cell-penetrating peptides (CPPs) to ELP[$V_5G_3A_2$-150] has on the polypeptide's solubility, structure, and aggregation properties. CPPs are known to enhance the uptake of ELP into cultured cells *in vitro* and into tumor tissue *in vivo*. Interestingly, the asymmetric addition of basic residues decreased the solubility of ELP[$V_5G_3A_2$-150], although below the T_T we still observed a low level of self-association that increased with temperature. The ΔH of the aggregation process correlates with solubility, suggesting that the basic CPPs stabilize the aggregated state. This is potentially beneficial as the decreased solubility will increase the fraction aggregated and enhance drug delivery efficacy at a heated tumor. Otherwise, the basic CPPs did not significantly alter the biophysical properties of ELP. All constructs were monomeric at low temperatures but self-associate with increasing temperature through an indefinite isodesmic association. This self-association was coupled to a structural transition to type II β-turns. All constructs reversibly aggregated in an endothermic reaction, consistent with a reaction driven by the release of water.

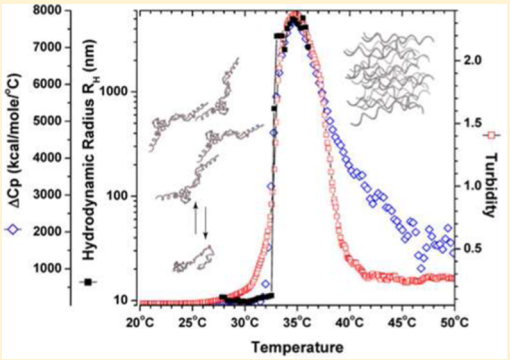

It was first observed in 1899[1] that isolated skeletal muscle reversibly contracts at high temperatures. This phenomenon was attributed to the contraction of elastin,[2] the main protein component of elastic tissues, at high temperatures.[3] Elastin is a nonpolar protein consisting of a repeating pentapeptide Val-Pro-Gly-Xaa-Gly (VPGXG) sequence, where the fourth residue, termed the guest residue, can be any amino acid other than proline. Elastin-like polypeptides (ELPs) are genetically engineered polypeptides that are derived from the physiological protein elastin and consist of the same pentapeptide repeats. ELPs also exhibit the hyperthermia-induced aggregation that is observed in endogenous elastin.[4] Urry extensively studied the aggregation process in ELPs and determined that at low temperatures ELP adopts a disordered, solvated structure. In response to hyperthermia, ELP undergoes a structural transition to a series of repeating type II β-turns, forming a β-spiral, and aggregates in a process driven by the hydrophobic effect.[3,5] The temperature at which the structural transition and aggregation occur is now termed the transition temperature (T_T).[6] The T_T is inversely related to both the hydrophobicity of the guest residue and the number of pentapeptide repeats.[7] The identity of the guest residue is commonly adjusted to control the overall hydrophobicity and, therefore, the T_T of a specific ELP.[6]

The thermoresponsive properties of ELP are currently being explored as a potential means of physically targeting systemically delivered drugs, with the hypothesis that a precisely engineered ELP will be soluble at physiological temperature (T_P) but will aggregate when an area, such as a tumor, is heated (T_H). The aggregation will therefore concentrate a systemically delivered ELP−drug conjugate to a heated tumor. This

Received: July 17, 2013
Revised: January 17, 2014
Published: January 22, 2014

hypothesis was originally explored in 2001[4,8,9] with an ELP sequence that was engineered to have a T_T greater than the physiological temperature but lower than the temperature of a heated tumor ($T_P < T_T < T_H$). This sequence was also engineered with a lysine residue for drug attachment (Lys-ELP1). Very promising results were obtained, and ELP has been used in more than 30 cell and animal studies to deliver small molecule drugs and peptide therapeutics to a variety of cancers, including brain tumors.[10] In many of these studies, cell-penetrating peptides (CPPs) were added to the N-terminal end of ELP to induce endocytosis and increase the level of tumor uptake.[11,12] Because of the lysine content of CPPs, this lysine residue was replaced with a cysteine (Cys-ELP) in these constructs to provide selectivity during labeling reactions.

We previously characterized Lys-ELP1[13] using a variety of complementary biophysical techniques to understand and predict its behavior as a drug delivery vector. It was determined that in solution at low temperatures (5 °C) and concentrations, Lys-ELP1 is monomeric and adopts an extended, disordered conformation with large f/f_o (2.88) and R_H (6.8−6.9 nm) values. As the temperature is increased, Lys-ELP1 exhibits weak association below the T_T that increased with temperature. The percent β-turn structure was observed by CD to increase with an increasing level of association. Above the T_T, a previously unreported critical concentration (C_C) that decreased with an increase in temperature was observed. This was in contrast with the predominant theory that ELP was soluble below the T_T and then became ordered and aggregated in an all-or-none manner. These results suggested that the concentration dependence of T_T is actually a measure of the solubility constant of ELP. This has important implications for understanding the behavior of ELP in serum as a drug delivery vector. Because ELP will not fully aggregate at the T_T, a constant concentration will circulate systemically below the T_T. In this study, we examine how the addition of basic CPPs affects the measured biophysical properties of ELP.

MATERIALS AND METHODS

Protein Purification. The constructs were designed *in silico* and constructed using standard molecular biology techniques on pUC19 and pET25b vectors. After confirmation of construct integrity by sequencing, the expression plasmids were transformed into *Escherichia coli* BLR(DE3) cells for protein expression. The expression strains were grown by innoculating a 500 mL sample of TB Dry medium with a 500 μL aliquot of bacterial culture and 2 mL of Amp. This culture was then grown for 18 h and then harvested using centrifugation (F9S-4X 1000Y, 5K rpm, 10 °C, 10 min). The bacterial pellet was resuspended in a small volume of 1× PBS, and this suspension was frozen at −80 °C until the protein was needed.

The frozen cell culture was thawed and lysed using sonication with six 10 s bursts at 70% amplitude interrupted by a 10 s pause. This mixture was centrifuged for 45 min at 13K rpm (Thermo Scientific, F21S 8X 50Y). The supernatant was collected and 1 mL of 10% PEI added to each tube (~35 mL) to precipitate negatively charged macromolecules. This solution was centrifuged for 30 min at 13K rpm. The supernatant was collected and filtered using vacumn filtration to remove any large impurities. The filtered solution was heated to 60 °C for 10 min to aggregate the ELP protein. The solution was centrifuged for 10 min at 10K rpm. This served to pellet and remove the ELP protein from the solution but leave the remainder of the soluble proteins in solution.

The protein was further purified to >99% purity through four rounds of thermal cycling. One thermal cycle consists of resuspending the pelleted protein into fresh 1× PBS by cooling the solution on ice. The solution is then spun for 2 min to pellet any large impurities. The supernatant is then transferred to a fresh tube and the tube heated in a water bath at 60 °C for 5 min and spun in a tabletop microcentrifuge, and the supernatant is discarded. This cycle is repeated three more times to fully purify the protein. When the protein is fully purified, the pellet should be completely translucent in the aggregated state. Certain constructs (Bac-Cys-ELP1) will have a slight yellowish tint; however, SynB1-Cys-ELP1 and Cys-ELP1 are completely clear, and the only differentiation between the solution and aggregated protein is the visible refractive index change. At the end of the purification, there are no observable contaminants on an sodium dodecyl sulfate−polyacrylamide gel electrophoresis, although in AUC absorbance experiments at 280 nm there was a small raised baseline observed. Therefore, the protein was always equilibrated into fresh buffer using the spun column method of Penefsky.[14]

Analytical Ultracentrifugation. All analytical ultracentrifugation (AUC) experiments were performed using a Beckman XLA instrument retrofitted to include a fluorescence detection system (AU-FDS, AVIV Biomedical). For experiments using absorbance detection, data were acquired using Proteome (Beckman). For fluorescence detection experiments, the centrifuge parameters and data collection were controlled by AU-AOS (AVIV). The focal depth of the FDS laser was calibrated to the height of the sample, and not the calibration cell, to improve the linearity of the measured plateau.[15] The meniscus position for all fluorescence experiments was determined by taking four intensity scans using the absorbance detection system after the run was complete. The intensity scans were then analyzed in DCDT2+[16] to select the correct meniscus. All experiments were performed using Spin-Analytical sedimentation velocity cells with 1.2 cm centerpieces at 50K rpm. The temperature of the AUC was calibrated using the method of Li and Stafford,[17] so that 5, 10, 20, 30, and 35 °C correspond to 4.62, 9.65, 19.69, 29.73, and 34.76 °C, respectively. After the samples had been loaded into the centrifuge, the temperature was equilibrated for at least 1 h prior to starting the sedimentation.

The density of the buffer was measured at each temperature using an Anton Parr DMA 5000 densitometer. The partial specific volume and buffer viscosity at each temperature were estimated using SedNTerp.[18] Sedimentation velocity data were analyzed with DCDT2+[16,19] both to choose an objective meniscus position and to produce a $g(s^*)$ sedimentation coefficient distribution. The data were analyzed with Sedfit[20] to produce a continuous $c(s^*)$ distribution up to 30 S to look for any stronger association that may have been missed by a $g(s^*)$ analysis. For isodesmic K_{iso} (M^{-1}) fitting, the data were imported into SEDANAL[21] for direct boundary analysis.

Protein Labeling with Fluorescein. To use the fluorescence detection system, all three constructs were covalently labeled with the small fluorescent dye fluorescein. The purified protein (stock solutions kept at ≈2 mM) was dissolved to a concentration of 100 μM in $NaCO_3$ buffer. A small amount of fluorescein-5-EX succinimidyl ester (Life Technologies) was dissolved in DMSO and the concentration determined by absorbance measurement of a dilution in

Table 1. Introduction to Construct Sequences and a Summary of Basic Properties[a]

Abbreviated Sequences	
Lys-ELP1	N′-MS-K-GPG(VPG[VGAVVVGAGV]G)$_{150}$WP-C′
Cys-ELP1	N′-M-C-GPG(VPG[VGAVVVGAGV]G)$_{150}$WP-C′
Bac-Cys-ELP1	N′-M-RRIRPRPPRLPRPRPRPLPFPRPG-C-GPG(VPG[VGAVVVGAGV]G)$_{150}$WP-C′
SynB1-Cys-ELP1	N′-M-RFFRLSYSRRRFSTSTGR-C-GPG(VPG[VGAVVVGAGV]G)$_{150}$WP-C′

Molecular Parameters									
	N	MW (Da)	pI	extinction coefficient (M^{-1} cm^{-1})	average disorder	$\langle H \rangle$	charge at pH 7	R_H, compact (nm)	R_H, unfolded (nm)
Lys-ELP1	758	59546.61	8.875	5690	0.9902	0.5894	0.69	3.26	8.88
Cys-ELP1	757	59337.39	5.622	5690	0.9902	0.5905	−0.31	3.25	8.75
Bac-Cys-ELP1	781	62397.16	12.544	5690	0.9901	0.5830	8.69	3.29	9.57
SynB1-Cys-ELP1	775	61739.16	12.002	6970	0.9901	0.5866	5.69	3.27	9.17

[a]The MW, pI, charge at pH 7, and extinction coefficient were calculated from the amino acid sequence using SedNTerp.[18] N is the total number of residues. The average disorder measures the probability of disorder on a scale of 0 (highly ordered) to 1 (no predicted order) using PONDR. The mean hydrophobicity was calculated from the amino acid sequence using the method of Kyte and Doolittle.[23] The hydrodynamic radius for a compact or unfolded shape was calculated as explained in the text.[25]

$NaCO_3$ buffer. The dissolved fluorescein-5-EX succinimidyl ester was added to the protein solution to achieve a final protein:dye ratio of 1:6. The reaction was allowed to proceed for 2 h at room temperature. To facilitate the reaction, the mixture was placed on a slowly rotating turntable. The reaction was stopped by performing three thermal cycles to remove free dye. To fully equilibrate the protein back into PBS buffer from the $NaCO_3$ buffer, the final cold supernatant was passed over a Penefsky column.[14] An amino specific probe is used rather than a Cys acting fluorescent probe to allow labeling of both sites in future experiments with drugs like paclitaxel and doxorubicin.

Dynamic Light Scattering. Prior to DLS measurements, an ELP stock solution was diluted to the appropriate concentration and 200 μL of the diluted sample was used to overfill the 10 μL volume DLS quartz cuvette. The DLS cuvette was inspected for air bubbles; if any were present, the cuvette was emptied and refilled. After the cuvette had been placed in the DLS instrument (DynaProTM NanoStar, Wyatt Technology), the temperature was allowed to equilibrate for 5 min. All DLS data were collected at 658 nm using a 10 s acquisition time. The data were typically collected at 1 °C intervals from 5 to 60 °C, although repeat measurements were collected at 0.25 °C to estimate uncertainties in R_H values at 5−6 °C and to avoid temperature overshoot effects near T_T (see Results). At each temperature, the system was equilibrated for approximately 2 min prior to measurement. The laser power was set to 50%; the autoattenuation mode was disabled, and the hydrodynamic radius values, R_H, were analyzed in regularization mode. The data were analyzed using DYNAMICS version 7.1.0, which was included with the instrument.

Differential Scanning Calorimetry. All DSC experiments were performed using a Microcal (Northampton, MA) VP-DSC instrument. For all experiments, both the sample and reference cells were filled with the appropriate buffer for baseline calibration, and the sample cell was refilled with the appropriate ELP solution. The protocol was set to ramp the temperature from 283 to 343 K (10−70 °C) at a rate of 1 °C/min and then rapidly cool the solution to 10 °C over 5 min. This was repeated twice to examine the reversibility of the ELP phase transition. Enthalpy ΔH was calculated by integrating the baseline-corrected excess heat capacity signal from 10 °C on either side of the phase change.

Turbidity. All turbidity measurements were performed using a Cary 100 Bio UV−vis spectrophotometer with an external Peltier temperature controller and a 1 cm path length cuvette. The temperature was monitored using a probe that was placed inside a reference cuvette. The accuracy of the probe was verified by using an external temperature probe to manually check the temperature over a range of 20−60 °C. To measure the T_T, the temperature was ramped at a rate of 0.1 °C/min. To examine the reversibility of aggregation, the temperature was ramped from 20 to 50 °C at a rate of 1 °C/min. The increase in rate was necessary as ELP forms aggregates above the T_T that will pellet under the force of gravity. The T_T was calculated by taking the derivative of the heating profile.

Circular Dichroism. All circular dichroism data were collected in a Jasco 720 instrument with a Jasco model PTC-423S single-position Peltier attachment controller using a 0.1 mm path length cuvette. Data were collected on each construct at two concentrations (0.75 and 1.25 mg/mL). At each concentration, three spectra were recorded and averaged at 10 °C intervals from 5 to 65 °C. The ellipticity at 196 nm was also measured at 1 °C intervals from 5 to 65 °C to compare the effect of temperature and concentration on β-turn formation.

RESULTS

Analysis of Protein Sequences. The sequences of the three constructs examined in this study are summarized in Table 1. For reference, the sequence of Lys-ELP1, the construct previously analyzed,[13] is also presented. These constructs have a cysteine residue located at the N-terminal end of ELP.[6,22] This results in approximately 30−50% of the population existing as disulfide-linked dimers as measured by sedimentation velocity [SV (data not shown)]. Thus, all biophysical measurements were initially performed in the presence of 1 mM TCEP. The cysteine is engineered solely to covalently attach small molecule drugs and, therefore, during treatments will be occupied by therapeutics and not available for disulfide-linked dimers.[12] Serum contains glutathione reductase and other reducing agents; therefore, any remaining disulfides should, in principle, be reduced. By examining the biophysical properties of the reduced constructs, we can examine the contributions caused by the modifications without the added complication of the MW increasing due to the presence of disulfide-linked dimers.[7]

The MW and mean hydrophobicity ($\langle H \rangle$)[23] of all constructs are similar, with all MWs consistent with each other within 5% (Table 1). We previously calculated the compaction index (CI)

dx.doi.org/10.1021/bi400955w | Biochemistry 2014, 53, 1081−1091

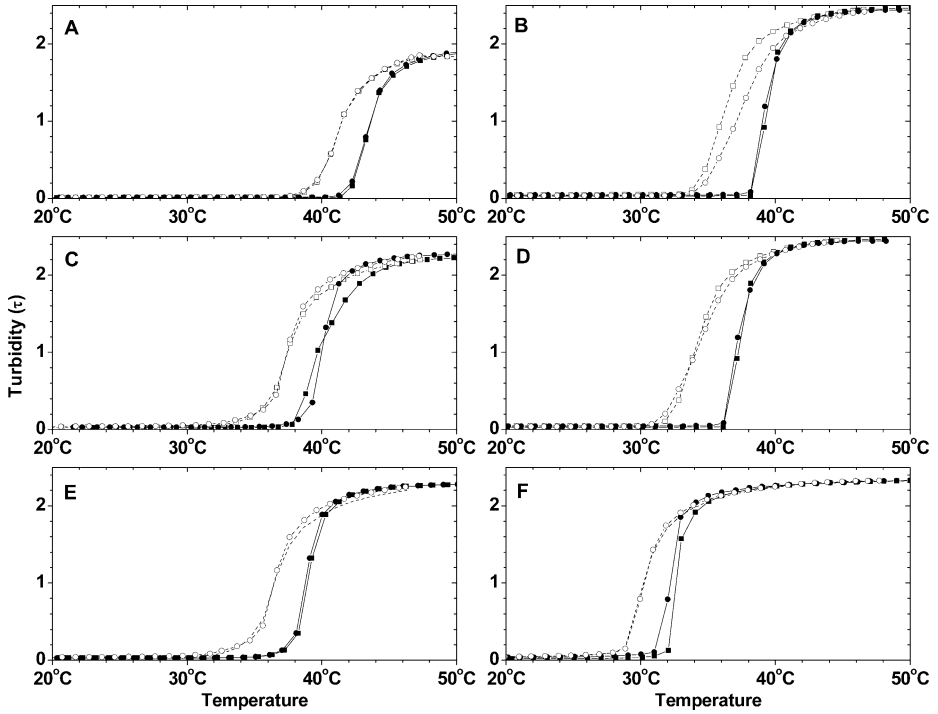

Figure 1. Testing the ability of constructs to reversibly aggregate. A 50 μM solution was heated and cooled at a rate of 1.0 °C/min. The solution was heated from 20 to 50 °C (■), cooled (□), reheated to 50 °C (●), and then cooled (○). (A) Cys-ELP1 in 1× PBS and 1 mM TCEP. (B) Cys-ELP1 in 95% FBS. (C) Bac-Cys-ELP1 in 1× PBS and 1 mM TCEP. (D) Bac-Cys-ELP1 in 95% FBS. (E) SynB1-Cys-ELP1 in 1× PBS and 1 mM TCEP. (F) SynB1-Cys-ELP1 in 95% FBS. All constructs reversibly aggregate in both PBS and FBS.

of ELP by calculating the hydrodynamic radius of a polypeptide of the same MW of ELP adopting either a globular or unfolded conformation and compared these values to the hydrodynamic radius of ELP measured by DLS and SV. The hydrodynamic radius (R_H) of a globular protein was calculated using the simple power law:[24]

$$R_H = R_0 N^{\nu} \quad (1)$$

where N is the total number of residues and R_0 and ν are constants determined by Wilkins et al.[24] (R_0 = 4.75, and ν = 0.29). The expected hydrodynamic radius for intrinsically disordered proteins with a high proline content was calculated using the formula described by Marsh and Forman-Kay:[25]

$$R_H = (AP_{pro} + B)(C|Q| + D)S_{His} \times R_0 N_{\nu} \quad (2)$$

where Q is the charge, P_{pro} is the fraction of prolines, S_{His} = 1 because no histidine tag is present, and A, B, C, D, R_0, and ν are constants (A = 1.24, B = 0.904, C = 0.00759, D = 0.963, R_0 = 2.49, and ν = 0.285, 0.549, or 0.509 for the folded, denatured, or IDP state, respectively).

The MW, $\langle H \rangle$, and calculated hydrodynamic radius of all constructs are essentially unchanged by the substitution of a lysine with a cysteine or the addition of CPPs. However, because the lysine residue contributed the only charge present at physiological pH, the overall charge and polarity are changed by modifications involving charged residues. At physiological pH, Lys-ELP1 has an overall calculated charge of 0.69. Replacement of the lysine residue with a cysteine lowers the overall calculated charge to −0.31. The addition of Bac or SynB1 raises the overall calculated charge to 8.68 or 5.68, respectively, at pH 7. It is important to note that the addition of CPPs to the N-terminal end also results in an asymmetric charge distribution.

Because of the overall charge at physiological pH, we expected to observe a change in the solubility of the ELP constructs. We hypothesized that as the magnitude of the overall charge increased, the solubility might correspondingly increase because of interactions with the solvent in the soluble state. This would be observed as an increase in the T_T. This obviously neglects the potential affect of asymmetric charge and stabilization of the aggregated state. To test this hypothesis, we performed solubility measurements.

Effect of CPPs on ELP Solubility and Reversibility. The use of ELP as a drug delivery vector is fundamentally dependent upon the construct remaining soluble at normal physiological temperatures (T_P) but reversibly aggregating at therapeutically attainable heated temperatures (T_H, i.e., $T_P < T_T < T_H$).[4,6,8,13] Therefore, there are two major questions. (1) Do the modified constructs retain the ability to thermally aggregate in a reversible manner? (2) How do the modifications affect the T_T?

The reversibility of ELP aggregation for all three constructs was examined in PBS and 95% FBS by heating and cooling a solution of 50 μM ELP and monitoring the turbidity[8,9] (Figure 1). For all constructs, the aggregation was observed to be reversible and repeatable in both PBS and 95% FBS. The effect of the basic CPPs on the T_T was examined by measuring the T_T as a function of concentration for each construct. For all constructs, the T_T was observed to decrease linearly with the logarithm of the ELP concentration. The results were plotted on a logarithmic concentration scale and fit using linear least-squares regression (LLSR) (Figure 2 and Table S1 of the Supporting Information). Note that by fitting the data on a logarithmic micromolar scale, the reported y-intercept is the T_T at 1 μM. All constructs exhibit similar trends between buffer conditions. The T_T in PBS and in 95% FBS is increased by

dx.doi.org/10.1021/bi400955w | *Biochemistry* 2014, 53, 1081−1091

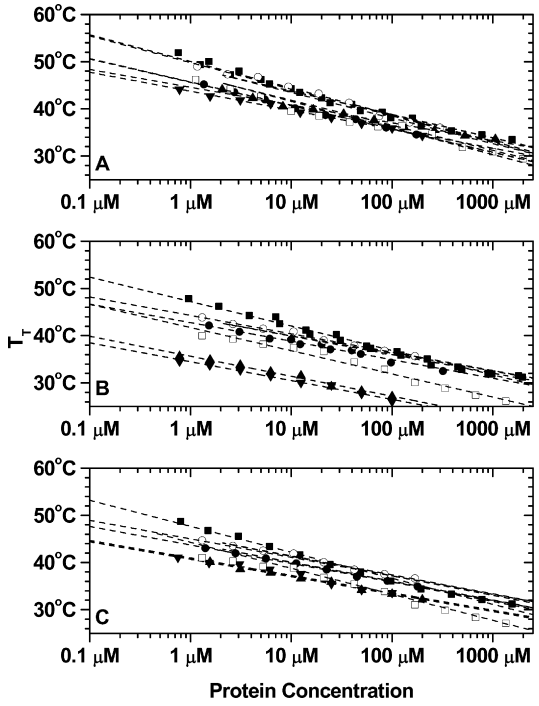

Figure 2. Measuring the T_T as a function of concentration: (A) Cys-ELP1, (B) Bac-Cys-ELP1, and (C) SynB1-Cys-ELP1. For each construct, the T_T was measured as a function of concentration in PBS (□), FBS (○), PBS with 1 mM TCEP (■), FBS with 1 mM TCEP (●), the sample labeled with fluorescein in PBS with 1 mM TCEP (▲), and the sample labeled with fluorescein in FBS (▼). The concentration dependence of the T_T was fit using LLSR and is summarized in Table S1 of the Supporting Information.

approximately 4 °C with the addition of TCEP. This trend is expected because it has been demonstrated that the T_T of ELP is inversely related to the MW.[7] Therefore, the reduction of disulfide-linked dimers by TCEP serves to lower the average MW and increase the T_T. Another interesting possible explanation is that the disulfide-linked dimers are serving as "early" nuclei and nucleating the aggregation process, similar to the nucleation of microtubules[26] or Hb-S.[27] The T_T is increased by approximately 1 °C in 95% FBS compared to PBS. Because macromolecular crowding would be expected to lower the T_T,[28] this suggests that all ELP constructs could be weakly associating with serum components. This trend is consistent with the results obtained for Lys-ELP.[13] All constructs exhibit a significant decrease (approximately 4 °C) in the T_T when they are covalently labeled with fluorescein (approximately 5–10% labeling efficiency), consistent with previous analyses.[4,13]

The observed decrease in solubility with an increase in charge is opposite of the hypothesized effect. The asymmetric addition of basic residues could be lowering the solubility of ELP in two ways; either the charges are decreasing the stability of the soluble state, or the aggregated state is being stabilized. The addition of asymmetric charges could be causing the ELP polymers to adopt a more extended conformation in the soluble state. This would cause an increase in the surface area exposed to solvent and a decrease in the number of intrachain (van der Waals) interactions. This would serve to decrease the energy required to aggregate the ELP polymers by decreasing the intrachain interactions broken or increasing the entropic gain of the interaction and thus be observed as a decrease in the T_T. This hypothesis would be supported by an increase in the hydrodynamic radius below the T_T. Alternatively, it is possible that the asymmetric charges are stabilizing the aggregated state. Similar to the formation of micellar structures, this could be through orienting the hydrophobic chains inward and leaving the polar CPPs exposed to solvent. To differentiate between these possibilities, we examined the hydrodynamic radius and enthalpy of the aggregation reaction by DLS and DSC.

Effect on Size and Thermodynamics. The hydrodynamic radius of each construct was measured as a function of temperature at three concentrations using DLS (Figure 3 and

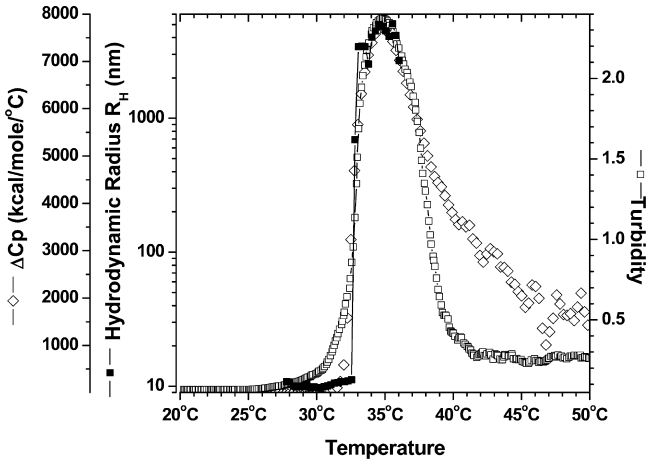

Figure 3. Examination of the aggregation process using DLS, DSC, and turbidity. This experiment was performed for three concentrations of each construct. Pictured are the results for 300 μM Synb1-Cys-ELP1. For each concentration, a 2 mL sample was prepared and 500 μL used for turbidity (□), 500 μL for DLS (■), and 1 mL for DSC (◇). All experiments were performed in PBS with 1 mM TCEP added. The results of this experiment and all others are summarized in Table 2. Note that the aggregates formed above the T_T will sediment to the bottom of the cuvette under the force of gravity. Because turbidity measurements were taken in the middle of the cuvette, the turbidity can be observed to decrease over time as the aggregates pellet. In DLS measurements, where the measurement is made at the bottom of the cuvette, this effect is attenuated.

summarized in Table 2). All three constructs exhibit a hydrodynamic radius at 5 °C of approximately 6.4 nm and are consistent within experimental error of each other at each concentraion. Two of the constructs, Cys-ELP1 and SynB1-Cys-ELP1, and the control, Lys-ELP1, exhibit a significant increase in size as a function of concentration and temperature below the T_T. The Lys, Cys, and SynB1 constructs are significantly larger at 300 μM, approaching 11.4, 9.7, and 8.5 nm, respectively, just below the T_T. The size of the Bac-Cys construct increases with temperature but only slightly, from 6.5 to 6.7 to 6.9 nm, with concentration. At and above the T_T, all constructs aggregate and form large particles that are approximately 2.5 orders of magnitude larger than those below the T_T.

The hydrodynamic radius observed in these experiments for all three constructs is slightly shorter than that observed for Lys-ELP (Table 2). This indicates that each construct is adopting a more compacted conformation than Lys-ELP (see Discussion). This suggests that the decrease in T_T observed is not caused by ELP adopting a more extended conformation where the level of intrachain interactions is decreased and the solvent-exposed surface area is increased. These data also suggest that ELP is not forming small spherical micelles, as

dx.doi.org/10.1021/bi400955w | Biochemistry 2014, 53, 1081–1091

Table 2. Summary of the DLS and DSC Data for Each ELP Construct[a]

construct	concn (μM)	R_H (nm) at 5 °C	R_H (nm) below the T_T	R_H (μm) above the T_T	ΔH (kcal/mol)
Lys-ELP1	130	6.95 ± 0.13	8.60 ± 1.09	2.32 ± 0.39	46.4
	260	6.87 ± 0.20	9.40 ± 0.32	2.67 ± 0.46	45.5
	390	6.77 ± 0.12	11.45 ± 0.67	2.39 ± 0.84	45.7
Cys-ELP1	150	6.34 ± 0.27	6.92 ± 0.16	2.47 ± 0.54	50.0
	300	6.49 ± 0.70	8.69 ± 0.55	2.78 ± 0.65	49.9
	450	6.43 ± 0.42	9.81 ± 1.69	2.43 ± 0.36	50.9
Bac-Cys-ELP1	100	6.23 ± 0.38	6.55 ± 0.22	3.18 ± 0.46	39.0
	200	6.54 ± 0.15	6.74 ± 0.24	3.11 ± 0.10	37.1
	300	6.60 ± 0.18	6.92 ± 0.09	3.88 ± 0.34	38.0
SynB1-ELP1	100	6.13 ± 0.76	6.67 ± 0.11	3.70 ± 0.38	44.0
	200	6.50 ± 0.72	7.76 ± 0.12	4.09 ± 0.28	45.6
	300	6.67 ± 0.12	8.55 ± 0.16	3.93 ± 0.29	44.5

[a]The DLS data are presented at temperatures below and above the T_T. The DSC data exhibit no concentration dependence, and average values are plotted in Figure 4 vs T_T at 1 μM.

these would be observed in the DLS data as intermediate sizes between monomers and the fully aggregated state.[29]

The change in enthalpy of the reaction was measured using DSC as a function of temperature at three concentrations (Figure 3 and summarized in Table 2). Consistent with the measurements on Lys-ELP, the aggregation reaction for each construct is endothermic and, over the concentration range examined, concentration-independent. The transition from the weakly associated state to the aggregated state must involve a similar cooperative process that does not reflect the fraction of weakly associated molecules. This may simply mean the weakly associated state is highly solvated or not a significant fraction of the total protein.

The enthalpy of Cys-ELP1 is 50.3 kcal/mol (averaged over the three concentrations measured). This is greater than the enthalpy previously measured for Lys-ELP1 (45.9 kcal/mol). As the overall charge is increased by the addition of the SynB1 and Bac CPP, the enthalpy decreases to 44.7 and 38.0 kcal/mol, respectively. The magnitude of the enthalpy exhibits an inverse correlation with the T_T extrapolated to a concentration of 1 μM (Figure 4). This correlation supports the hypothesis that the decrease in the solubility is due to the stabilization of the assembled state with an increase in charge density. This suggests that the asymmetric charges are orienting to the exterior of the aggregates, and therefore, more water remains bound. It will be very interesting to see if this trend holds for additional ELP constructs with different overall charge densities.

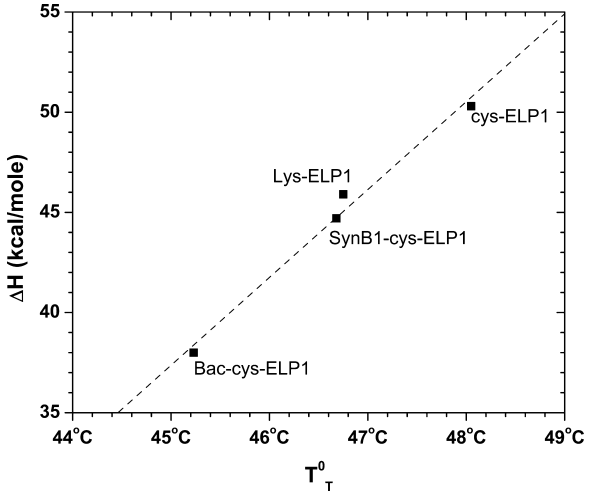

Figure 4. Plot of enthalpy as a function of T_T. For each construct, the enthalpy was measured at three concentrations ranging from approximately 100 μM to approximately 450 μM and appeared, over this concentration range, to be concentration-independent. Therefore, the enthalpy presented here is the average enthalpy of each construct. The $T°_T$ presented is the transition temperature at protein concentration of 1 μM. The linear fit has an R^2 of 0.986.

Effect on Secondary Structure. The secondary structure of each construct was examined using circular dichroism as a function of temperature and concentration (Figure 5). The spectra measured are essentially identical to the CD structure that was obtained for Lys-ELP1[13] and CD spectra on ELPs of different lengths and guest residue compositions.[30−33] All three constructs exhibit the same spectral features (Figure 5A−C). At low temperatures, there is a minimum at approximately 195 nm that is characteristic of a random or disordered polypeptide structure.[34] At high temperatures, there is a maximum at approximately 210 nm that is characteristic of type II β-turns.[35] The magnitude of the minimum at 195 nm decreases with an increase in temperature (Figure 5D). The magnitude of the 195 nm minima also decreases with an increase in concentration (Figure 5D), suggesting that weak self-association is occurring and that this association promotes ordered β-turn structures. This weak self-association below the T_T is also observed in the DLS data as an increase in the hydrodynamic radius with an increase in temperature. These results are consistent with the biophysical properties of Lys-ELP1. The increase in the maximum at approximately 210 nm with an increase in temperature is consistent with increasing percent β-turn conformation. All three constructs exhibit virtually identical molar ellipticities and temperature dependencies, suggesting that the addition of CPPs is not affecting the secondary structure of the majority of the polypeptide. The quantitative deconvolution of the CD spectra into specific structural elements is difficult because no satisfactory reference set exists for IDPs. Current efforts are focused on collecting laser Raman data to complement CD data and quantitatively estimate secondary structures, along with molecular dynamics simulations. Preliminary Raman data collected on 200 μM Lys-ELP1 show predominantly β-turn and very little or no random coil (J. Benevides, data not shown), consistent with a concentration-dependent folding of ELP below the T_T.

Examining the Hydrodynamic Properties. In our previous study of Lys-ELP1, we quantified the weak self-

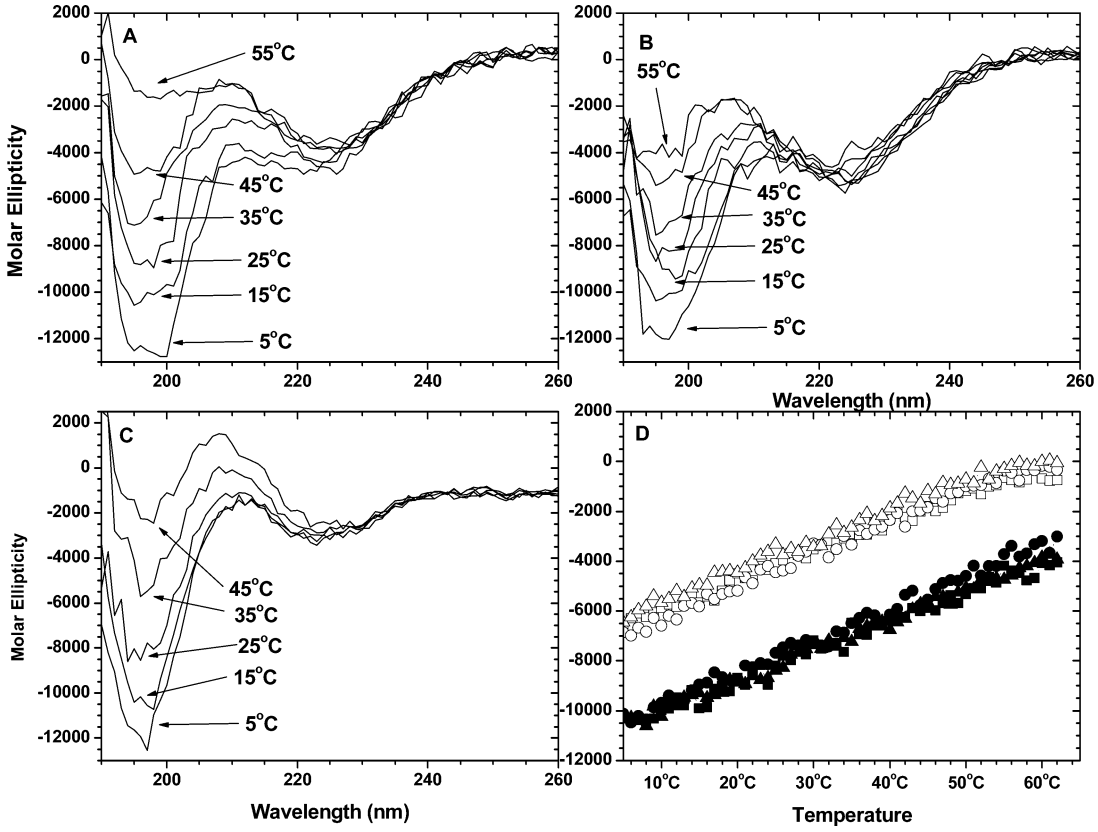

Figure 5. Examination of the secondary structure using circular dichroism. (A) CD spectra of 0.64 mg/mL Cys-ELP1 and 1 mM TCEP in PBS as a function of temperature. (B) CD spectra of 0.71 mg/mL Bac-Cys-ELP1 and 1 mM TCEP in PBS as a function of temperature. (C) CD spectra of 0.69 mg/mL SynB1-Cys-ELP1 and 1 mM TCEP in PBS as a function of temperature. (D) Temperature dependence of the magnitude of the molar ellipticity at 196 nm plotted for Cys-ELP1 (■), Bac-Cys-ELP1 (●), and SynB1-Cys-ELP1 (▲). The ellipticity was also measured at 1.4 mg/mL (empty symbols).

association observed in the DLS and CD data by performing SV analysis. We found that at a low temperature (5 °C) Lys-ELP1 behaved as an extended, nonideal monomer. As the temperature was increased, the $s^{\circ}_{20,w}$ increased, consistent with self-association. By globally fitting all of the raw data obtained at five temperatures, we determined that the association was best explained by an indefinite isodesmic association model. This suggested that no distinct stable species were formed (i.e., trimers, pentamers, etc.) but the association was best described as indefinite with a constant K_{iso} between each step. We hypothesized that the three constructs examined here should exhibit the same properties (i.e., indefinite, isodesmic association that is enhanced with an increase in temperature) exhibited by Lys-ELP1. Furthermore, we hypothesized that the magnitude of the association should be inversely related to the extrapolated T_T (i.e., as the solubility decreases, we would observe a greater strength of association at each temperature). This suggests a connection among weak association, possible nucleation, inversion temperature, and phase change.

The sedimentation coefficient of all three constructs examined in this study decreases with concentration at 5 °C (Figure 6 and summarized in Table S2 of the Supporting Information). This is caused by hydrodynamic nonideality and is consistent with the behavior observed with Lys-ELP1, an extended protein with a large excluded volume. The f/f_o values at 5 °C are 2.86, 2.90, and 2.89, consistent with an extended shape. The extrapolated sedimentation coefficients ($s^{\circ}_{20,w}$) were used to calculate the R_H values for each construct (7.46 nm for Cys, 7.70 nm for Bac, and 7.64 nm for SynB1). The R_H values measured by SV are similar but ~16% larger than the R_H values measured by DLS [~6.4 nm on average (Table 2)]. To further address this discrepancy, DLS data were repeated at 300 μM and a finer (0.25 °C) temperature spacing, and the low-temperature data (5, 5.25, 5.5, and 5.75 °C) were averaged. The data were consistent among the constructs (Lys, 6.78 ± 0.22 °C; Cys, 6.89 ± 0.30 °C; Bac, 7.02 ± 0.81 °C; SynB1, 6.80 ± 0.76 °C) and consistently smaller than the SV estimates, although within one or two standard deviations of the mean. A major difference between the DLS and SV data is that the s values are extrapolated to zero ELP concentration, while these DLS data above are measured at 100−450 μM. Thus, the discrepancy, an ~10% lower R_H value derived from these more precise DLS measurements versus SV, may be due to a concentration or nonideality effect. To resolve this discrepancy, we collected DLS data at 5 °C on the SynB1 form at 2, 4, 6, and 8 mg/mL (32−128 μM) and extrapolated to 0 °C. However, there was no upward trend, and the extrapolated R_H values are consistent with the previous measurements. Given the scatter in the DLS measurements (data above and Table 2), we must conclude a large uncertainty and not nonideality is the cause of this apparent discrepancy.

For all Cys constructs, the magnitude of the apparent nonideality (K_s or the apparent slope) observed in the SV experiments decreases with an increase in temperature (Figure 6), consistent with weak self-association occurring below the T_T. At each temperature, there is no significant difference in the

dx.doi.org/10.1021/bi400955w | Biochemistry 2014, 53, 1081−1091

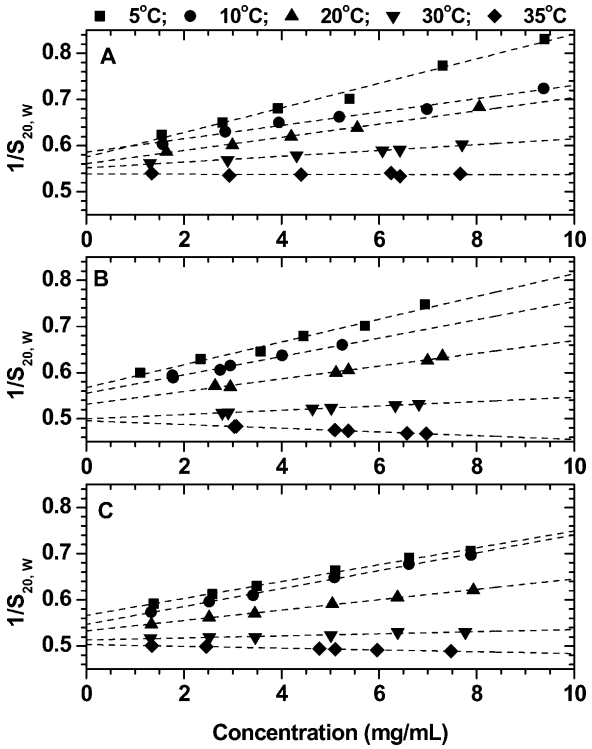

Figure 6. Examining the hydrodynamic properties of polypeptide constructs. The sedimentation coefficient for each construct was measured as a function of concentration and temperature and plotted as $1/s$ vs c mg/mL to extract apparent K_s and extrapolated f/f_o values: (A) Cys-ELP1 and 1 mM TCEP in PBS, (B) Bac-Cys-ELP1 and 1 mM TCEP in PBS, and (C) SynB1-Cys-ELP1 and 1 mM TCEP in PBS. The decrease in the sedimentation coefficient with concentration at low temperatures is caused by hydrodynamic nonideality. As the temperature is increased, the magnitude of the apparent K_s is decreased as weak self-association masks the nonideality. The nonideal isodesmic sedimentation analysis with Sedanal is summarized in Table 3.

hydrodynamic properties among the three constructs (Table S2 of the Supporting Information), suggesting that the addition of a Bac or SynB1 CPP has a minimal effect on the hydrodynamic properties of ELP ($s_{20,w}$, K_s, and f/f_0).

The raw SV data from each temperature were fit to indefinite, isodesmic association models (summarized in Table 3). The hydrodynamic properties at 5 °C were used to define baseline, nonassociative properties of ELP. It was assumed, as described previously,[13] that there is no change in the shape or nonideality with an increase in temperature. This is a reasonable starting point because all the f/f_o values for each Cys construct and temperature examined are between 2.53 and 2.90. This allows us to attribute all of the temperature-dependent change in the concentration dependence to weak self-association. At 10 °C, all constructs demonstrate virtually the same extent of self-association, −3.59 ± 0.03 kcal/mol. This trend continues with an increase in temperature (−4.24 ± 0.07 kcal/mol at 20 °C, −4.88 ± 0.19 kcal/mol at 30 °C, and −5.30 ± 0.19 kcal/mol at 35 °C), although Bac-ELP1 and SynB1-ELP1 exhibit a slightly greater extent of association than Cys-ELP1. These values are consistent with the Lys-ELP1 data as a function of temperature (−3.30, −4.41, −5.17, and −5.58 kcal/mol), although the K_{iso} values of the Lys construct are consistently larger at higher temperatures. To test the hypothesis that self-association is linked to the phase change,

Table 3. Summary of Global Isodesmic Fitting of SV Data at Each Temperature for Each Cys-ELP Construct[a]

	K_{iso} (M^{-1})		
	Cys-ELP1	Bac-Cys-ELP1	SynB1-Cys-ELP1
	10 °C		
best fit	6.07×10^2	5.52×10^2	5.97×10^2
95% confidence interval	$\langle 5.93 \times 10^2, 6.21 \times 10^2 \rangle$	$\langle 5.22 \times 10^2, 5.81 \times 10^2 \rangle$	$\langle 5.78 \times 10^2, 6.12 \times 10^2 \rangle$
standard deviation	0.00821	0.00446	0.00578
	20 °C		
best fit	1.61×10^3	1.29×10^3	1.48×10^3
95% confidence interval	$\langle 1.58 \times 10^3, 1.64 \times 10^3 \rangle$	$\langle 1.27 \times 10^3, 1.30 \times 10^3 \rangle$	$\langle 1.21 \times 10^3, 1.73 \times 10^3 \rangle$
standard deviation	0.00452	0.00499	0.00537
	30 °C		
best fit	2.30×10^3	4.08×10^3	3.75×10^3
95% confidence interval	$\langle 2.20 \times 10^3, 2.41 \times 10^3 \rangle$	$\langle 4.06 \times 10^3, 4.10 \times 10^3 \rangle$	$\langle 3.48 \times 10^2, 3.89 \times 10^2 \rangle$
standard deviation	0.00644	0.00536	0.00593
	35 °C		
best fit	4.11×10^3	7.50×10^3	6.03×10^3
95% confidence interval	$\langle 4.09 \times 10^3, 4.13 \times 10^3 \rangle$	$\langle 7.47 \times 10^3, 7.54 \times 10^3 \rangle$	$\langle 5.79 \times 10^3, 6.21 \times 10^3 \rangle$
standard deviation	0.00588	0.00626	0.00513

[a]The uncertainties in K_{iso} were determined by Fstat at a 95% confidence interval.

these data are compared with the T_T data for PBS in Table S1 of the Supporting Information. Note that the absence of TCEP lowers the extrapolated $T°_T$ for all three Cys constructs in PBS, consistent with a role for cross-linked dimers (increased MW) affecting aggregation. The $T°_T$ data with TCEP follow the trend of 48.05, 45.23, and 46.68 °C for Cys, Bac, and SynB constructs, respectively. While this is consistent with our hypothesis, it does not prove the suggestion that these weak complexes nucleate or are directly involved in the aggregation or phase change process. The data for Lys-ELP1 reveal slightly more association at 35 °C (−5.58 kcal/mol) but a higher T_T (46.75 °C). Thus, additional factors like stabilization of large aggregates must play a role.

Serum Analyses. In an attempt to study the hydrodynamic properties in serum, all constructs were fluorescently labeled with fluorescein (abbreviated F-construct) and sedimented at varying levels of FBS. All data sets exhibited the J−O or Johnston−Ogston effect,[13,36−38] a classic boundary sharpening anomally caused by high concentrations of other components. All three constructs demonstrate a decrease in the weight average sedimentation coefficient with an increase in the level of FBS (Figure S1 of the Supporting Information). This is attributed to hydrodynamic nonideality and indicates that none of the constructs are forming strong associations with serum components, which would be observed as an increase in the sedimentation coefficient with concentration. Separate investigations do suggest that ELP weakly associates with some IgG component(s) (manuscript in preparation). As the temperature is increased to 30 °C, the magnitude of the apparent nonideality in serum decreases. This is consistent with the temperature-dependent behavior observed in PBS and suggests that ELP also exhibits weak association in serum.

dx.doi.org/10.1021/bi400955w | Biochemistry 2014, 53, 1081−1091

DISCUSSION

In this study, the structural, thermodynamic, and hydrodynamic properties of three ELP derivatives being investigated for drug delivery are presented. These constructs are designed to deliver drugs through systemic delivery at physiological temperatures, where the drug−ELP conjugates will be soluble, and subsequent localization is achieved through the use of applied heat. The polypeptides vary from the construct previously examined (Lys-ELP1) by the replacement of a lysine residue with a cysteine to the subsequent addition of either a Bac or SynB1 CPP to the N-terminus. The cysteine residue was engineered for the attachment of small drugs through thiol−ether linkages, and the CPPs provide enhanced uptake into tumor cells by induction of endocytosis. There are two specific questions to be investigated. (1) What are the effects of CPP modifications on the biophysical properties? (2) Will these changes impact the therapeutic role of ELPs as a drug delivery vector?

The reversibility of thermal aggregation was investigated for all three constructs in PBS and FBS and found to be completely reversible. The T_T was then examined as a function of concentration. Consistent with previous results, the T_T was a linear function of the logarithm of the concentration. Surprisingly, the replacement of lysine with a cysteine increased the T_T by 1.30 °C, which is the opposite of the expected effect, as removing the only charge would have been expected to lower the solubility. This trend was continued as adding charged CPPs, which was thought to increase the solubility, actually lowered the T_T for SynB1- and Bac-Cys-ELP1. This could be explained by the asymmetric charge addition either destabilizing the soluble state or stabilizing the aggregated state. The addition of asymmetric charges could be acting to lower the solubility by causing ELP to adopt a more extended conformation and expose more surface area to solvent. This hypothesis was explored by examining the hydrodynamic radius through the use of DLS and AUC. The hydrodynamic radii measured by SV for all constructs at 5 °C were similar to each other within experimental error and to that of the previously characterized Lys-ELP1 construct (6.92 nm for Lys, 7.46 nm for Cys, 7.70 nm for Bac, and 7.64 nm for SynB1).

Previously, we calculated the CI of Lys-ELP1 (0.349) using the method of Brocca et al.[39] The CI of each construct suggests a moderate compact conformation (0.424 for Cys-ELP, 0.464 for SynB1-Cys-ELP1, and 0.497 for Bac-Cys-ELP1), consistent with the high proline contents (~150/750 or 20%). This suggests that Cys-ELPs are not on average adopting a fully extended conformation and that the decrease in the T_T is caused by the addition of charges making the aggregated state more stable. The aggregated state may become more ordered where the hydrophobic regions are buried and the polar regions are left exposed to solvent, similar to a micelle formation. This is supported by the decrease in the ΔH observed with a decrease in $T°_T$. Future studies will examine the role of water release during the phase change by titrating with osmolytes to lower water activity. (Preliminary data for the SynB1 form suggest 50 ± 5 water molecules are released during the phase change.)

The effect on the structural and hydrodynamic properties was examined by CD and SV. In our previous analysis of Lys-ELP1, we observed weak association that became stronger with an increase in temperature. This weak association appeared to cause an increase in the level of β-turn structure. These analyses suggested that the T_T of ELPs is more accurately described as a solubility constant, where the increase in temperature causes ELP to undergo a structural transition to an ordered structure. These same biophysical properties were observed for all three constructs. Weak association below the T_T was observed in both the DLS data, through an increase in the hydrodynamic radius with temperature, and the CD data, through a decrease in the magnitude of the minima at 195 nm. The magnitude of the ellipticity is the same as that observed for the Lys-ELP1 construct, which suggests that the CPP addition has a minimal effect on the secondary structure. SV was used to quantify the extent of the association observed below the T_T. The strength of the association correlated with the T_T, where a lower T_T suggested an increased level of association occurring in the sample, although the Lys construct does not follow the same quantitative trend as the Cys constructs. When Cys-ELP1 was sedimented in serum, two important features were observed. Consistent with a previous study, the sedimentation coefficient decreases with an increase in the level of FBS. This suggests that none of the constructs are forming strong associations with serum components, which would be observed as an increase in the sedimentation coefficient with an increase in concentration. Second, the magnitude of the nonideality decreases with an increase in temperature. This suggests that all constructs are still exhibiting weak association below the T_T, consistent with the behavior in PBS.

It is worth noting that the simple idea of a disordered to ordered transition is too simple to describe the data because the loss of disorder and the formation of β-turn occur with an increase in concentration (see CD data) and an increase in temperature below the T_T. Laser Raman data collected on a 200 uM sample (J. Benevides, to be presented elsewhere) reveal very little disordered structure and exclusively β-turn. The concentration dependence of SV and DLS data suggests this structural transition is coupled to weak association. This is in part the basis of the idea that these weak complexes may serve as nuclei for the phase change. Other factors may play a role, for example, a more concerted release of water, the formation of a more ordered β-spiral, and more extensive or stabilized condensation or coacervate formation. The nature of the weak association is not known in part because ELPs lack a definite structure that might be used for docking experiments. One could imagine random hydrophobic intermolecular interactions along many regions of each molecule that statistically sum to a weak isodesmic complex. This model would predict complexes with similar nonideality per gram, an assumption of our isodesmic fitting, if the monomers in these weak complexes retained the same degree of compaction. Future experiments and simulations will attempt to test these hypotheses.

The goal of this research is to examine the biophysical properties of CPP−ELP constructs and how the behavior as a drug delivery vector might be affected. Modifying the construct to replace a lysine residue with a cysteine was performed to provide greater selectivity in the presence of basic CPPs. The addition of the basic CPPs is designed to induce endocytosis and enhance drug delivery. In a concentration- and buffer-dependent manner, one could ask how these modifications affect the solubility and delivery of aggregated protein. This comparison can be calculated from the fits summarized in Table S1 of the Supporting Information. For example, in PBS at 42 °C, the soluble concentrations are 9.8 μM for Lys-ELP, 11.8 μM for Cys-ELP, 1.4 μM for Bac-ELP, and 1.3 μM for SynB1-ELP. The Cys constructs are tested in 1 mM TCEP to avoid

disulfide formation effects. In 95% FBS at 42 °C, the soluble concentrations are 27.3 μM for Lys-ELP, 8.6 μM for Cys-ELP, 4.2 μM for Bac-ELP, and 7.1 μM for SynB1-ELP. In general, the Cys constructs are similar to or slightly better than the Lys-ELP construct in terms of their effect on solubility.[a] As discussed previously, these trends clearly have consequences for dosage and therapeutic delivery,[13] although we must stress the importance of directly testing the influence of physiologic buffers and drug labeling on T_T and solubility. In general, the biophysical properties (SV, CD, DLS, and DSC) are not significantly affected by these modifications. Furthermore, from a therapeutic and pharmagological perspective, the dose and clinical efficiacy must still be evaluated empirically for different drugs and tumor models.

We are continuing our biophysical analyses in three directions: (1) optimizing ELP as a drug delivery vector, (2) elucidating the mechanism of the aggregation process, and (3) quantitative analysis of the hydrodynamic properties of ELPs in serum. ELP has been precisely engineered so that $T_P < T_T < T_H$. Our analyses suggest that the aggregation of ELPs is more accurately defined as a solubility constant; therefore, a low concentration will circulate systemically and not aggregate above the T_T. With a decrease in the MW of the polymer, and an increase in the hydrophobicity, the T_T can remain in the ideal range while lowering the concentration that will circulate systemically. In addition, we demonstrate for the first time a significant correlation between the transition temperature and the enthalpy of the reaction. We are in the process of examining the role of water in the aggregation process by repeating our analyses as a function of osmolyte concentration. This should allow us to quantify the relationship between the T_T and the enthalpy of the reaction. We are also complementing our use of CD with laser Raman spectroscopy to examine the secondary structure of aggregated ELP. Finally, we have been investigating the hydrodynamic properties in serum and have been able to accurately describe the sedimentation properties of ELP in physiological concentrations of BSA and IgG (manuscript in preparation). Our current investigations will attempt to elucidate the role of lipids and fatty acids alone and bound to albumin, with the goal of systematically characterizing all the major components of serum so that the hydrodynamic properties can be quantitatively investigated. How this impacts drug delivery and whether it is improved by altering the CPP–ELP sequence are the questions.

■ ASSOCIATED CONTENT

Supporting Information

Fitting of T_T versus log(C) (Table S1), fitting of $1/s_{20,w}$ versus concentration (Table S2), and $1/s_{20,w}$ data as a function of the level of FBS (Figure S1). This material is available free of charge via the Internet at http://pubs.acs.org.

■ AUTHOR INFORMATION

Corresponding Author

*Department of Biochemistry, University of Mississippi Medical Center, 2500 N. State St., Jackson, MS 39216. E-mail: jcorreia@umc.edu. Phone: (601) 984-1502.

Funding

Supported by the UMC AUC Facility, National Science Foundation (NSF) Major Research Instrumentation Grant 1040372 to J.J.C., and NSF Grant CBET-0931041 to D.R. W.H.K. acknowledges financial support by the Mississippi INBRE, funded by an Institutional Development Award from the National Institute of General Medical Sciences of the National Institutes of Health via Grant P20GM103476.

Notes

The authors declare the following competing financial interest(s): D.R. owns a company called TTT that is funded by an SBIR grant.

■ ABBREVIATIONS

CD, circular dichroism; Cc, critical concentration; CPP, cell-penetrating peptide; DLS, dynamic light scattering; DSC, differential scanning calorimetry; ELP, elastin-like polypeptide; f/f_o, frictional coefficient ratio; J–O, Johnston–Ogston; R_H, radius of hydration; SV, sedimentation velocity; T_T, transition temperature.

■ ADDITIONAL NOTE

[a]A concern with lowering the solubility concentration is that it may promote aggregation at off-targets. Off-target accumulation is unavoidable, and this is being extensively studied in the Raucher lab by various whole animal scanning methods. Previous work has described the occurrence of ELP occlusions that block blood flow in the extremeties. The appropriate approach to dealing with this situation would be to test various doses to find an effective and safe dose.

■ REFERENCES

(1) Brodie, T. G., and Richardson, S. W. F. (1899) A study of the phenomena and causation of heat contraction of skeletal muscle. *Philos. Trans. R. Soc. London 191*, 127–146.

(2) McCartney, J. E. (1913) Heat Contraction of Elastic Tissue. *Exp. Physiol. 7*, 103–114.

(3) Urry, D. W. (1992) Free Energy Transduction in Polypeptides Based on Inverse Temperature Transitions. *Prog. Biophys. Mol. Biol. 57*, 23–57.

(4) Meyer, D. E., Kong, G. A., Dewhirst, M. W., Zalutsky, M. R., and Chilkoti, A. (2001) Targeting a Genetically Engineered Elastin-like Polypeptide to Solid Tumors by Local Hyperthermia. *Cancer Res. 61*, 1548–1554.

(5) Reguera, J., Urry, D. W., Parker, T. M., McPherson, D. T., and Rodríguez-Cabello, J. C. (2007) Effect of NaCl on the Exothermic and Endothermic Components of the Inverse Temperature Transition of a Model Elastin-like Polymer. *Biomacromolecules 8*, 354–358.

(6) Chilkoti, A., Dreher, M. R., Meyer, D. E., and Raucher, D. (2002) Targeted drug delivery by thermally responsive polymers. *Adv. Drug Delivery Rev. 54*, 613–630.

(7) Meyer, D. E., and Chilkoti, A. (2004) Quantification of the Effects of Chain Length and Concentration on the Thermal Behavior of Elastin-like Polypeptides. *Biomacromolecules 5*, 846–851.

(8) Meyer, D. E., Shin, B. C., Kong, G. A., Dewhirst, M. W., and Chilkoti, A. (2001) Drug targeting using thermally responsive polymers and local hyperthermia. *J. Controlled Release 74*, 213–224.

(9) Raucher, D., and Chilkoti, A. (2001) Enhanced Uptake of a Thermally Responsive Polypeptide by Tumor Cells in Response to Its Hyperthermia-mediated Phase Transition. *Cancer Res. 61*, 7163–7170.

(10) Hearst, S. M., Walker, L. R., Shao, Q., Lopez, M., and Raucher, D. (2011) The design and delivery of a thermally responsive peptide to inhibit S100B-mediated neurodegeneration. *Neuroscience 197*, 369–380.

(11) Bidwell, G. L., and Raucher, D. (2005) Application of thermally responsive polypeptides directed against c-Myc transcriptional function for cancer therapy. *Mol. Cancer Ther. 4*, 1076–1085.

(12) Massodi, I., Bidwell, G., III, and Raucher, D. (2005) Evaluation of cell penetrating peptides fused to elastin-like polypeptide for drug delivery. *J. Controlled Release 108*, 396–408.

(13) Lyons, D. F., Le, V., Bidwell, G. L., III, Kramer, W. H., Lewis, E. A., Raucher, D., and Correia, J. J. (2013) Structural and Hydrodynamic Analysis of a Novel Drug Delivery Vector: ELP[$V_5G_3A_2$-150]. *Biophys. J. 104*, 2009−2021.
(14) Penefsky, H. S. (1979) A centrifuge-column procedure for the measurement of ligand binding by beef heart F1. *Methods Enzymol. 56*, 527−530.
(15) Lyons, D. F., Lary, J. W., Husain, B., Correia, J. J., and Cole, J. L. (2013) Are fluorescence-detected sedimentation velocity data reliable? *Anal. Biochem. 437*, 133−137.
(16) Philo, J. S. (2006) Improved methods for fitting sedimentation coefficient distributions derived by time-derivative techniques. *Anal. Biochem. 354*, 238−246.
(17) Liu, S., and Stafford, W. F. (1995) An optical thermometer for direct measurement of cell temperature in the Beckman instruments XL-A analytical ultracentrifuge. *Anal. Biochem. 224*, 199−202.
(18) Laue, T. M., Shah, B. D., Ridgeway, R. M., and Pelletier, S. M. (1992) Analytical Ultracentrifugation in Biochemistry and Polymer Science. In *Computer-aided Interpretation of Analytical Sedimentation Data For Proteins* (Harding, S. E., Rowe, A. J., and Horton, J. C., Eds.) pp 90−125, The Royal Society of Chemistry, Cambridge, U.K.
(19) Stafford, W. F. (1992) Boundary Analysis in Sedimentation Transport Experiments: A Procedure for Obtaining Sedimentation Coefficient Distributions Using the Time Derivative of the Concentration Profile. *Anal. Biochem. 203*, 295−301.
(20) Schuck, P. (1998) Sedimentation Analysis of Noninteracting and Self-Associating Solutes Using Numerical Solutions to the Lamm Equation. *Biophys. J. 75*, 1503−1512.
(21) Stafford, W. F., and Sherwood, P. J. (2004) Analysis of heterologous interacting systems by sedimentation velocity: Curve fitting algorithms for estimation of sedimentation coefficients, equilibrium and kinetic constants. *Biophys. Chem. 108*, 231−243.
(22) Meyer, D. E., and Chilkoti, A. (2002) Genetically encoded synthesis of protein-based polymers with precisely specified molecular weight and sequence by recursive directional ligation: Examples from the elastine-like polypeptide system. *Biomacromolecules 3*, 357−367.
(23) Kyte, J., and Doolittle, R. F. (1982) A Simple Method for Displaying the Hydropathic Character of a Protein. *J. Mol. Biol. 157*, 105−132.
(24) Wilkins, D. K., Grimshaw, S. B., Receveur, V., and Dobson, C. M. (1999) Hydrodynamic radii of native and denatured proteins measured by pulse field gradient NMR techniques. *Biochemistry 38*, 16424−16431.
(25) Marsh, J. A., and Forman-Kay, J. D. (2010) Sequence Determinants of Compaction in Intrinsically Disordered Proteins. *Biophys. J. 98*, 2383−2390.
(26) Vulevic, B., and Correia, J. J. (1997) Thermodynamic and Structural Analysis of Microtubule Assembly: The Role of GTP Hydrolysis. *Biophys. J.*, 1357−1375.
(27) Magdoff-Fairchild, B., Poillon, W. N., Li, T., and Bertles, J. F. (1976) Thermodyanmic studies of polymerization of deoxygenated sickle cell hemoglobin. *Proc. Natl. Acad. Sci. U.S.A. 73*, 990−994.
(28) Ellis, R. J. (2001) Macromolecular crowding: Obvious but underappreciated. *Trends Biochem. Sci. 26*, 597−604.
(29) Furgeson, D. Y., Dreher, M. R., and Chilkoti, A. (2006) Structural optimization of a "smart" doxorubicin−polypeptide conjugate for thermally targeted delivery to solid tumors. *J. Controlled Release 110*, 362−369.
(30) Nicolini, C., Ravindra, R., Ludolph, B., and Winter, R. (2004) Characterization of the Temperature- and Pressure-Induced Inverse and Reentrant Transition of the Minimum Elastin-like Polypeptide GVG(VPGVG) by DSC, PPC, CD, and FT-IR Spectroscopy. *Biophys. J. 86*, 1385−1392.
(31) Gross, P. C., Possart, W., and Zeppezauer, M. (2003) An Alternative Structure Model for the Polypentapeptide in Elastin. *Z. Naturforsch., C: J. Biosci. 58*, 873−878.
(32) Reiersen, H., Clarke, A. R., and Rees, A. R. (1998) Short Elastin-like Peptides Exhibit the Same Temperature-induced Structural Transitions as Elastin Polymers: Implications for Protein Engineering. *J. Mol. Biol. 283*, 255−264.
(33) Urry, D. W., Shaw, R. G., and Prasad, K. U. (1985) Polypentapeptide of elastin: Temperature dependence of ellipticity and correlation with elastomeric force. *Biochem. Biophys. Res. Commun. 130*, 50−57.
(34) Martin, S. R., and Schilstra, M. J. (2008) Circular dichroism and its application to the study of biomolecules. *Methods Cell Biol. 84*, 263−293.
(35) Woody, R. W. (1995) Circular dichroism. *Methods Enzymol. 246*, 34−71.
(36) Johnston, J. P., and Ogston, A. G. (1946) A boundary anomaly found in the ultracentrifugal sedimentation of mixtures. *Trans. Faraday Soc. 42*, 789−799.
(37) Harrington, W. F., and Schachman, H. K. (1953) Analysis of a Concentration Anomaly in the Ultracentrifugation of Mixtures. *J. Am. Chem. Soc. 75*, 3533−3539.
(38) Trautman, R., Schumaker, V. N., Harrington, W. F., and Schachman, H. K. (1954) The Determination of Concentration in the Ultracentrifugation of Two-Component Systems. *J. Chem. Phys. 22*, 555−559.
(39) Brocca, S., Testa, L., Sobott, F., Šamalikova, M., Natalello, A., Papaleo, E., Lotti, M., De Gioia, L., Doglia, S. M., Alberghina, L., and Grandori, R. (2011) Compaction Properties of an Intrinsically Disordered Protein: Sic1 and Its Kinase-Inhibitor Domain. *Biophys. J. 100*, 2243−2252.